# Electron mean-free-path calculations using a model dielectric function

David R. Penn
*National Bureau of Standards, Gaithersburg, Maryland 20899*
(Received 18 June 1986)

The inelastic electron mean free path as a function of energy is calculated for Cu, Ag, Au, and Al. The calculations are based on a model dielectric function $\epsilon(q,\omega)$, which is obtained from a modification of the statistical approximation. In this approach $\epsilon(0,\omega)$ is determined by the experimentally measured optical dielectric function. Calculated mean free paths are compared to experimental data and to other theories.

## I. INTRODUCTION

The inelastic electron mean free path (MFP) plays an important role in surface physics. It is required for quantitative surface analysis by Auger electron spectroscopy and x-ray photoemission spectroscopy and determines the surface sensitivity of photoemission experiments. Moreover, the MFP plays a role in the interpretation of almost any experiment in which an excited electron moves through a solid, for example, low-energy electron diffraction, bremsstrahlung isochromat spectroscopy, etc. Despite the importance of the inelastic MFP, experimental values for a given material are generally available only in a limited energy range and the measured values are subject to uncertainties due to difficulties associated with the experiments. On the theoretical side the situation is no better. With the exception of free-electron materials such as Al, the MFP has not been calculated from first principles. The primary missing ingredient is the dielectric response function which depends on the energy and momentum lost by an electron in a collision. Thus, existing calculations are semiphenomenological and, because of experimental problems, it is difficult to assess how well the theories actually work.

In this paper a method is proposed for calculating the MFP based on a model dielectric function whose form is motivated by the use of the statistical approximation. This approximation was first applied to MFP calculations by Tung *et al.*[1] who approximated the MFP directly rather than the dielectric function. In the limit that the momentum transfer is zero, the model dielectric function is set equal to the measured optical dielectric function which is presently available for a wide variety of materials largely from synchrotron radiation studies. The idea of using optical data in MFP calculations was first introduced by Powell.[2] Our results are calculated values of the MFP for electron energies in the range of 5 to $10^4$ eV.

## II. THEORY

The MFP for an electron of energy $E_k=\hbar^2k^2/2m$ in a free-electron gas is

$$\lambda_L(k;r_s)=\left[\frac{\hbar k}{m}\right]\left[\frac{\hbar}{2|M_I(k;r_s)|}\right], \tag{1}$$

where $r_s$ is the average distance between valence electrons in units of the Bohr radius $a_0$, and $r_s=(\frac{3}{4}\pi n)^{1/3}a_0^{-1}$, where $n$ is the electron density. The imaginary part of the electron self-energy is given by Quinn[3] as

$$M_I(k;r_s)=-\frac{e^2}{2\pi^2}\int\frac{d^3q}{q^2}\mathrm{Im}\frac{1}{\epsilon_L(q,E_{\mathbf{k}}-E_{\mathbf{k}-\mathbf{q}};r_s)}\,,$$
$$E_{\mathbf{k}}\geq E_{\mathbf{k}-\mathbf{q}}\geq E_F\,, \tag{2}$$

where $E_F$ is the Fermi energy and $\epsilon_L$ is the Lindhard dielectric function. This approximation neglects the vertex correction, self-consistency, and exchange and correlation, but gives reasonable values for the MFP in free-electron-like materials.[4] A free-electron-like material is one in which the loss function $-\mathrm{Im}[1/\epsilon(q=0,\omega)]$, as determined from optical or electron-energy-loss experiments shows a predominant peak due to well-defined volume plasmons which have an energy close to the free-electron value $\omega_p=(4\pi ne^2/m)^{1/2}$.

The dielectric function has not been calculated from first principles for non-free-electron metals such as the transition and noble metals. Consequently, Eq. (2) cannot be employed to determine the MFP. Tung *et al.*[1] have used the statistical approximation developed by Lindhard and co-workers[5] to calculate the MFP. The statistical approximation as applied to calculating the electron MFP assumes that the inelastic scattering of an electron in a volume element $d^3r$ of the solid can be approximated by the scattering appropriate to a free-electron gas of the electron density $n(r)$, in that volume element. Thus, the statistical approximation gives the inverse MFP as

$$\lambda^{-1}(k)=\int\frac{d^3r}{\Omega}\lambda_L^{-1}(k;r_s(r))\,, \tag{3a}$$

where

$$r_s(r)=[\tfrac{3}{4}\pi n(r)]^{1/3}a_0^{-1} \tag{3b}$$

and the region of integration in Eq. (3a) is a Wigner-Seitz cell of volume $\Omega$. For simplicity, the charge distribution is assumed to be spherically symmetric and the Wigner-Seitz cell is replaced by a sphere of volume $\Omega$.

In order to take advantage of the generally available values of $\epsilon(\omega)$, the experimentally determined optical dielectric function, the response function of the material

under consideration $\epsilon(q,\omega)$ is approximated rather than $\lambda^{-1}(k)$. In analogy with Eq. (3a) it is assumed that

$$\mathrm{Im}\frac{1}{\epsilon(q,\omega)}=\int\frac{d^3r}{\Omega}\mathrm{Im}\frac{1}{\epsilon_L(q,\omega;r_s^p(\omega))}\ , \tag{4a}$$

where

$$r_s^p(r)=[\tfrac{3}{4}\pi n_p(r)]^{1/3}a_0^{-1}\ . \tag{4b}$$

Here, $n_p(r)$ is a pseudo-charge-density chosen to ensure that

$$\mathrm{Im}\frac{1}{\epsilon(0,\omega)}=\mathrm{Im}\frac{1}{\epsilon(\omega)}\ . \tag{5}$$

Use of

$$\mathrm{Im}\frac{1}{\epsilon_L(0,\omega;r_s^p(r))}=-\frac{\pi}{2}\omega_p(r)\delta(\omega-\omega_p(r))\ , \tag{6a}$$

where

$$\omega_p(r)=\left[\frac{4\pi e^2}{m}n_p(r)\right]^{1/2} \tag{6b}$$

and Eq. (4a) in Eq. (5) yields

$$\mathrm{Im}\frac{1}{\epsilon(\omega)}=-\frac{2\pi^2}{\Omega}\left.\frac{r^2\omega}{[\partial\omega_p(r)/\partial r]}\right|_{\omega=\omega_p(r)}\ . \tag{7}$$

Equation (7) determines $\omega_p(r)$ and hence $n_p(r)$. It is possible to proceed without actually finding $n_p(r)$. The integration variable in Eq. (4a) is changed from $r$ to $\omega_p(r)$ to obtain

$$\mathrm{Im}\frac{1}{\epsilon(q,\omega)}=-\int_0^\infty d\omega_p(r)r^2\frac{1}{[\partial\omega_p(r)/\partial r]}\times\mathrm{Im}\frac{1}{\epsilon_L(q,\omega;\omega_p(r))}\ , \tag{8}$$

where $\epsilon_L(q,\omega;\omega_p(r))\equiv\epsilon_L(q,\omega;r_s^p(r))$. Use of Eq. (7) in Eq. (8) yields the result

$$\mathrm{Im}\frac{1}{\epsilon(q,\omega)}=\int_0^\infty d\omega_p G(\omega_p)\mathrm{Im}\frac{1}{\epsilon_L(q,\omega;\omega_p)}\ , \tag{9a}$$

where

$$G(\omega)=-\frac{2}{\pi\omega}\mathrm{Im}\frac{1}{\epsilon(\omega)}\ . \tag{9b}$$

Thus, a knowledge of the optical dielectric function $\epsilon(\omega)$ is sufficient to obtain $\mathrm{Im}[1/\epsilon(q,\omega)]$. It is trivial to show that the $f$ sum rule is satisfied

$$\int_0^\infty d\omega\,\omega\,\mathrm{Im}\frac{1}{\epsilon(q,\omega)}=-\frac{\pi}{2}\frac{4\pi Ne^2}{m}\ , \tag{10}$$

where $N$ is the number of electrons per unit volume in the solid. It also follows directly from Eq. (9) that

$$\mathrm{Re}\frac{1}{\epsilon(q,\omega)}=1+\int_0^\infty\frac{d\omega'\,\omega'}{\omega'^2-\omega^2}\mathrm{Im}\frac{1}{\epsilon(q,\omega')}=\int_0^\infty d\omega_p G(\omega_p)\mathrm{Re}\frac{1}{\epsilon_L(q,\omega;\omega_p)}\ . \tag{11}$$

Obviously Eq. (9) can be obtained directly from the assumption that

$$\mathrm{Im}\frac{1}{\epsilon(q,\omega)}=\int_0^\infty d\omega_p g(\omega_p)\mathrm{Im}\frac{1}{\epsilon_L(q,\omega;\omega_p)}\ , \tag{12}$$

where $g$ is to be determined by the condition that Eq. (5) is satisfied. However, the statistical approximation serves to motivate the present approach.

The imaginary part of the self-energy is now obtained by replacing $\mathrm{Im}(1/\epsilon_L)$ in Eq. (2) by $\mathrm{Im}(1/\epsilon)$. The resultant equation can be written as

$$M_I(k)=-\frac{e^2}{2\pi^2}\int_0^{E_{\mathbf{k}}-E_F}d(\hbar\omega)\int\frac{d^3q}{q^2}\mathrm{Im}\frac{1}{\epsilon(q,\omega)}\times\delta(\hbar\omega-E_{\mathbf{k}}+E_{\mathbf{k}-\mathbf{q}})\ . \tag{13}$$

The condition

$$\hbar\omega=E_{\mathbf{k}}-E_{\mathbf{k}-\mathbf{q}} \tag{14}$$

restricts the region in $(\omega,q)$ space over which the integrations in Eq. (13) take place. Equation (14) describes a collision in which an electron of energy $E_{\mathbf{k}}$ makes a transition to the state $E_{\mathbf{k}-\mathbf{q}}$ and loses energy $\omega$. In this paper we assume that $E_{\mathbf{k}}$ and $E_{\mathbf{k}-\mathbf{q}}$ are free-electron-like. This assumption would fail for energies near $E_F$ in the case of transition metals because of the unfilled $d$ bands, but it is a reasonable approximation for the noble metals. Equation (14) then gives

$$\hbar\omega\le\frac{\hbar^2}{2m}(2kq-q^2)\ , \tag{15}$$

where $k$ is the initial momentum of the scattered electron.

Our expression for $\lambda^{-1}(k)$ obtained from Eq. (9) and Eq. (13) is *not* the same as that given by the statistical approximation as used by Tung *et al.*, Eq. (3), even when $n(r)$ in Eq. (3) is replaced by the pseudo charge density $n_p(r)$. This is because $E_F$ appearing in the upper limit of the integral in Eq. (13) denotes the Fermi energy of the actual material under consideration. To be more explicit, Eqs. (13) and (9) yield

$$M_I(k)=\int_0^\infty d\omega_p G(\omega_p)\frac{e^2}{2\pi^2}\int_0^{E_{\mathbf{k}}-E_F}d(\hbar\omega)\int\frac{d^3q}{q^2}\mathrm{Im}\frac{1}{\epsilon_L(q,\omega;\omega_p)}\delta(\hbar\omega-E_{\mathbf{k}}+E_{\mathbf{k}-\mathbf{q}})\ . \tag{16}$$

Only if $E_F$ appearing in the limit of the integral in Eq. (16) is replaced by $E_F(\omega_p)$, the Fermi energy of a free-electron gas with plasma frequency $\omega_p$, would our approximation to the MFP give the same results as using a pseudo density $n_p(r)$, in the approach of Tung *et al.*,[1] Eq. (3a).

The angular integrations in Eq. (16) are trivial and yield

$$M_I(k)=\int_0^\infty d\omega_p G(\omega_p)\left[\frac{1}{\pi a_0 k}\int_0^{E_k-E_F} d(\hbar\omega)\int_{q_-}^{q_+}\frac{dq}{q}\mathrm{Im}\left[\frac{1}{\epsilon_L(q,\omega;\omega_p)}\right]\right], \tag{17a}$$

$$q_\pm = k\left[1\pm\sqrt{1-(\hbar\omega/E_k)}\right]. \tag{17b}$$

We find empirically that when $E_k$ is 200 eV or greater the quantity $\mathrm{Im}(1/\epsilon_L)$ in Eq. (17a) can be replaced by the single-pole approximation with a resulting loss of accuracy in the computed MFP of less than 3%. The one-pole approximation is

$$\mathrm{Im}\frac{1}{\epsilon_L(q,\omega;\omega_p)} = -\frac{\pi}{2}\frac{\omega_p^2}{\omega_p(q)}\delta(\omega-\omega_p(q)), \tag{18a}$$

where

$$\omega_p^2(q)=\omega_p^2+\tfrac{1}{3}[v_F(\omega_p)q]^2+(\hbar q^2/2m)^2, \tag{18b}$$

where $v_F(\omega_p)$ is the fermi velocity of a free-electron gas with plasma frequency equal to $\omega_p$. Use of Eq. (18) in Eq. (17) yields

$$M_I(k)=\frac{1}{2\pi a_0 k}\int d(\hbar\omega_p)\mathrm{Im}\frac{1}{\epsilon(\omega_p)} \times\ln\left[\frac{\bar\omega_p+\bar\omega_p(q)}{\bar q^{\,2}}+\frac{2}{3\bar\omega_p}\right]\Bigg|_{\bar q_2}^{\bar q_1}, \tag{19}$$

where $\bar\omega_p=\omega_p/E_F$, $\bar q=q/k_F$, and $\bar\omega_p(q)^2=\bar\omega_p^2+\frac{4}{3}\bar q^{\,2}+\bar q^{\,4}$. The quantities $\bar q_1$, $\bar q_2$ in Eq. (19) depend on $\bar\omega_p$ and are the values of $\bar q$ for which $\bar\omega_p(\bar q)$ intersects the boundary of the region given by $\bar\omega<2\bar k\,\bar q-\bar q^{\,2}$ and $\bar\omega\le\bar k^{\,2}-1$ corresponding to the limits of integration of the second and third integrals in Eq. (17a). Analytic expressions for $\bar q_1$ and $\bar q_2$ are given in Appendix A. Thus, for energies $E_k$ above 200 eV the MFP can be found from Eq. (19) rather than Eq. (17) and only a single integration rather than a triple integration is required.

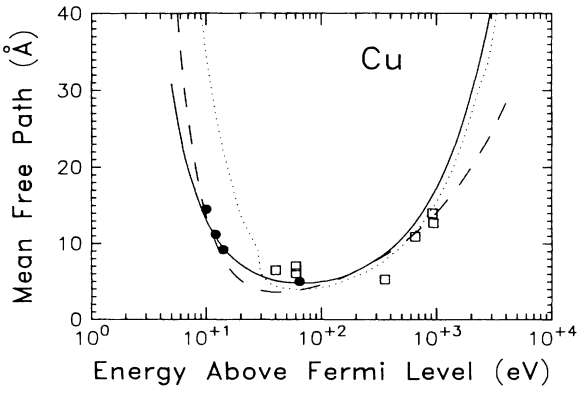


FIG. 1. Inelastic electron mean free path versus energy above the Fermi energy for Cu. Solid curve is present theory. Dotted curve is theory of Tung *et al.* (Ref. 1). Dashed curve is from Seah and Dench (Ref. 8). Experimental data: solid circles, Refs. 10 and 11; open squares, Ref. 14.

## III. RESULTS

The present theory, making use of experimental values of $\mathrm{Im}[1/\epsilon(\omega)]$ from Ref. 6, will be compared only with other theories that give the MFP for electrons of arbitrary energy. Several theories, all but one of which apply only to energies above 200 eV, have been compared in a detailed review by Powell.[7] There are only two previous theories that are applicable to both free and non-free-electron-like solids at both high and low electron energies, the statistical theory of Tung *et al.*[1] which we have discussed in detail, and a purely phenomenological theory by Seah and Dench.[8] The latter is based on fitting existing experimental data to a form $\lambda(E)=AE^{-2}+BE^{-1/2}$, where $A,B$ are determined from simple physical data. This work has been critiqued by Powell[7] and by Wagner *et al.*

Figures 1–4 as well as Table I show the MFP versus energy for Cu, Ag, Au, and Al, respectively. The results of various experiments are also indicated. Most of the data come from the overlayer type of experiment. An interesting exception is the MFP data for Cu by Knapp *et al.*[10] and by Himpsel *et al.*[11] that are obtained from photoemission line broadening. The theory of Tung *et al.*[1] gives rather large values for the MFP at low energies. This is because the $G_T(\omega)$ that would enter their theory [see Eq. (13) and the discussion following it] is derived from the true metallic charge density and for small values of $\omega$, $G_T(\omega)<(2/\pi\omega)\mathrm{Im}[1/\epsilon(\omega)]$. Thus, they predict less scattering than is dictated by Eq. (9b).

From the figures it appears that the theory of Tung *et al.*[1] gives values of the MFP that are too large at low energies and those given by the present theory are somewhat low, while that of Seah and Dench[8] gives values of

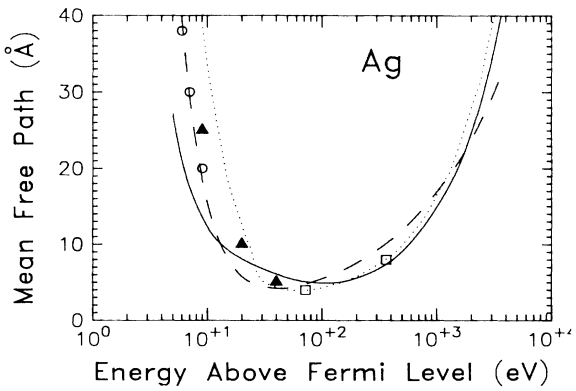


FIG. 2. Same as Fig. 1 but for Ag. Experimental data: open circles, Ref. 15; solid triangles, Ref. 16; open squares, Ref. 17.

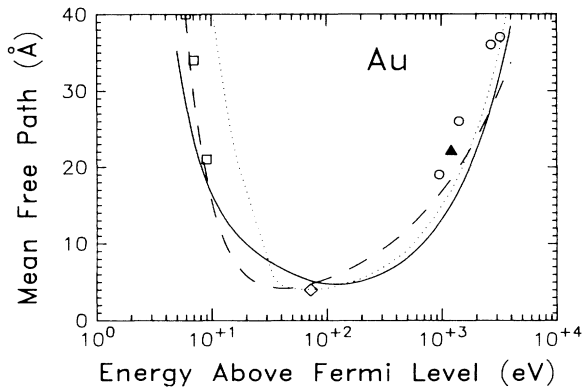


FIG. 3. Same as Fig. 1 but for Au. Experimental data: open squares, Ref. 15; open diamond, Ref. 17; open circles, Ref. 18; solid triangle, Ref. 19.

the MFP that are too low at high energies. Because of experimental difficulties there exists an uncertainty in the data that makes comparison of theory and experiment somewhat problematical. Also, the experimental values determined by the overlayer method (i.e., the values at high energies in Figs. 1—4) are not directly comparable to theory due to the effects of elastic electron scattering in these measurements.[7]

Our method depends on knowing the following: (1) the experimental values of $\mathrm{Im}[1/\epsilon(\omega)]$; (2) a knowledge of $E_F$ for the material; and (3) a free-electron-like band structure at energies above $E_F$. Assumption (1) can be relaxed under the following condition. If $\mathrm{Im}[1/\epsilon(\omega)]$ is known only up to some energy $\omega_{\max}$, then the theory still gives the MFP for energies less than or equal to $\omega_{\max}$. Items (2) and (3) are certainly important only for low electron energies, say, less than 50 eV. For cases such as transition metals where (3) fails, it may be possible to replace Eq. (15) by a more appropriate relationship. Based on secondary polarized-electron experiments and their interpretation,[12,13] it appears that, even for transition metals, Eq. (15) will not introduce any significant error as long as the electron energy is greater than 10 eV above the Fermi energy.

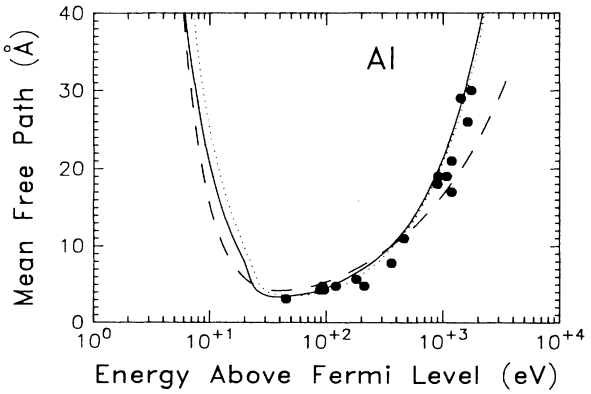


FIG. 4. Same as Fig. 1 but for Al. Experimental data: solid circles, Ref. 20.

TABLE I. Calculated electron MFP as a function of energy relative to the Fermi energy.

| $E$ (eV) | $\lambda_{Cu}$ (Å) | $\lambda_{Ag}$ (Å) | $\lambda_{Au}$ (Å) | $\lambda_{Al}$ (Å) |
|---|---|---|---|---|
| 5 | 30.8 | 27.1 | 35.2 | 53.9 |
| 6 | 23.9 | 21.0 | 28.4 | 41.3 |
| 7 | 19.7 | 17.6 | 23.5 | 33.4 |
| 8 | 17.0 | 15.3 | 20.3 | 28.0 |
| 9 | 14.8 | 13.6 | 18.0 | 23.7 |
| 10 | 13.1 | 12.3 | 16.4 | 20.6 |
| 15 | 8.9 | 9.3 | 11.9 | 11.9 |
| 20 | 7.2 | 8.1 | 9.9 | 7.8 |
| 40 | 5.1 | 6.1 | 6.8 | 3.4 |
| 60 | 4.8 | 5.3 | 5.6 | 3.7 |
| 80 | 4.8 | 5.0 | 5.0 | 4.1 |
| 100 | 5.0 | 4.9 | 4.8 | 4.6 |
| 150 | 5.6 | 5.1 | 4.8 | 5.9 |
| 200 | 6.4 | 5.6 | 5.2 | 7.0 |
| 500 | 10.7 | 9.1 | 8.2 | 12.7 |
| 1000 | 17.3 | 14.9 | 13.2 | 21.4 |
| 1500 | 23.5 | 19.8 | 17.8 | 29.4 |
| 2000 | 29.5 | 24.7 | 22.2 | 37.2 |
| 3000 | 40.8 | 34.1 | 30.4 | 52.0 |
| 4000 | 51.7 | 43.0 | 38.4 | 66.2 |
| 5000 | 62.2 | 51.7 | 46.1 | 79.9 |
| 10 000 | 111.7 | 92.5 | 82.2 | 144.9 |

There are two different sources of error in the present theory. The first type of error arises from the use of Eq. (13) for the self-energy. Equation (13) assumes the validity of the Born approximation, neglects the vertex correction, self-consistency, and exchange and correlation. At energies above 100 to 200 eV these effects are estimated to introduce errors on the order of 10% in the case of a free-electron gas.[4] At low energies the error is expected to be larger, particularly in view of the possible failure of the Born approximation. The second type of error comes from approximating the actual dielectric function by means of Eq. (9). Because the inelastic scattering is primarily in the forward direction at higher energies, Eq. (5) ensures a "reasonable" estimate of the MFP. However, the calculated MFP is sensitive to the momentum dependence of the dielectric function assumed in Eq. (9) which is dictated by the statistical approximation. Thus, the present theory is expected to be more accurate at high energies than at low energies, but it is difficult to estimate the degree of accuracy.

## APPENDIX A

The limits $q_1$ and $q_2$ in Eq. (19) are determined from the conditions

$$\bar{q}>0\,, \tag{A1a}$$

$$\bar{\omega}_p(\bar{q})=2\bar{k}\,\bar{q}-\bar{q}^2\,, \tag{A1b}$$

$$\bar{\omega}_p(\bar{q})=\bar{k}^2-1\,, \tag{A1c}$$

where

$$\bar{\omega}_p(\bar{q})=\bar{\omega}_p^2+\tfrac{4}{3}\bar{q}^2+\bar{q}^4\,. \tag{A1d}$$

Equation (A1b) has either no solutions or two solutions and Eq. (A1c) has one solution from $\bar{q} \geq 0$. The quantity $\bar{q}_1$ is the smallest solution of (A1b) and $\bar{q}_2$ is the smallest of the second solution of (A1b) and the solution of Eq. (A1c). Equations (A1b) and (A1d) give

$$\bar{q}^{\,3} - a_2 \bar{q}^{\,2} + a_0 = 0 , \tag{A2a}$$

where

$$a_0 = \bar{\omega}_p^2 / 4\bar{k} , \tag{A2b}$$

$$a_2 = \bar{k} - \left[ \frac{1}{3\bar{k}} \right] . \tag{A2c}$$

The solutions to Eq. (A2) for $(a_2/3)^2 > a_0/2$ are:

$$\bar{q}_a = \frac{a_2}{3} \left[ 1 - \cos\left[ \frac{\varphi}{3} \right] + \sqrt{3} \sin\left[ \frac{\varphi}{3} \right] \right] , \tag{A3a}$$

$$\bar{q}_b = \frac{a_2}{3} \left[ 1 + 2\cos\left[ \frac{\varphi}{3} \right] \right] , \tag{A3b}$$

and for $(a_2/3)^2 < a_0/2$:

$$\bar{q}_c = \frac{a_2}{3} \left[ 1 + \cos\left[ \frac{\varphi}{3} \right] - \sqrt{3} \sin\left[ \frac{\varphi}{3} \right] \right] , \tag{A3c}$$

$$\bar{q}_d = \frac{a_2}{3} \left[ 1 + \cos\left[ \frac{\varphi}{3} \right] + \sqrt{3} \sin\left[ \frac{\varphi}{3} \right] \right] , \tag{A3d}$$

where

$$\varphi = \tan^{-1} \left[ \frac{\{ a_0 [ (a_3/3)^3 - (a_0/4) ] \}^{1/2}}{| (a_2/3)^3 - (a_0/2) |} \right] . \tag{A3e}$$

Equation (A1c) has the solution

$$\bar{q}_e = ( -\tfrac{2}{3} + \{ (\tfrac{2}{3})^2 + [ (\bar{k}^{\,2} - 1) - \bar{\omega}_p^2 ] \}^{1/2} )^{1/2} . \tag{A4}$$

If $(a_2/3)^3 > a_0/3$ then $\bar{q}_1 = \bar{q}_a$ and $\bar{q}_2 = \min\{\bar{q}_b, \bar{q}_e\}$. If $(a_2/3)^3 < a_0/3$ then $\bar{q}_1 = \bar{q}_a$ and $\bar{q}_2 = \min\{\bar{q}_d, \bar{q}_e\}$.


[1] C. J. Tung, J. C. Ashley, and R. H. Ritchie, Surf. Sci. **81**, 427 (1979).

[2] C. J. Powell, Surf. Sci. **44**, 29 (1974).

[3] J. J. Quinn, Phys. Rev. **126**, 1453 (1962).

[4] D. R. Penn, Phys. Rev. B **13**, 5248 (1976).

[5] J. Linhard and M. Schraff, K. Dan. Vidensk. Selsk. Mat.-Fys. Medd. **27**, 15 (1953); J. Linhard, M. Schraff, and H. E. Schiott, *ibid.* **33**, 14 (1963).

[6] H. J. Hagemann, W. Gudat, and C. Kunz, Deutsches Elektronensynchrontron Report SR-74/7, 1974 (unpublished).

[7] C. J. Powell, Scanning Electron Microsc. **184**, 1649 (1984).

[8] M. P. Seah and W. A. Dench, Surf. Interface Anal. **1**, 2 (1979).

[9] C. D. Wagner, L. E. Davis, and W. M. Riggs, Surf. Interface Anal. **2**, 52 (1980).

[10] J. A. Knapp, F. J. Himpsel, and D. E. Eastmann, Phys. Rev. B **19**, 4952 (1979).

[11] F. J. Himpsel and W. E. Eberhardt, Solid State Commun. **31**, 747 (1979).

[12] D. Pines and P. Nozieres, *The Theory of Quantum Liquids* (Benjamin, New York, 1966), Vol. 1, p. 211.

[13] D. R. Penn, S. P. Apell, and S. M. Girvin, Phys. Rev. Lett. **55**, 518 (1985); Phys. Rev. B **32**, 7753 (1985).

[14] M. P. Seah, J. Phys. F **3**, 1538 (1973); Surf. Sci. **32**, 703 (1972).

[15] H. Kanter, Phys. Rev. **81**, 2357 (1970).

[16] D. E. Eastman, quoted by J. C. Tracy, NATO Summer School, on Induced Electron Emission, Ghent, 1972 (unpublished).

[17] P. W. Palmberg and T. N. Rhodin, J. Appl. Phys. **39**, 2425 (1968).

[18] M. Klasson, J. Hedman, A. Berndtsson, R. Nilsson, and C. Nordling, Phys. Scr. **5**, 93 (1972).

[19] Y. Baer, P. F. Heden, J. Hedmann, M. Klasson, and C. Nordling, Solid State Commun. **8**, 1479 (1970).

[20] J. C. Tracy, J. Vac. Soc. Tech. **11**, 280 (1974); C. J. Powell, Surface Interface Anal. **7**, 256 (1985).